APPLIED ORGANOMETALLIC CHEMISTRY
*Appl. Organometal. Chem.* 2001; **15**: 344–351
DOI: 10.1002/aoc.165

# Synthesis and characterization of poly(*N*-vinylpyrrolidone) filled by monodispersed silver clusters with controlled size†

G. Carotenuto
Institute of Composite Materials Technology, National Research Council, Piazzale Tecchio 80, 80125 Naples, Italy

**Dispersions of very small metal particles in polymeric matrixes are scientifically and technologically important. Here, poly(*N*-vinylpyrrolidone) (PVP) filled with nanometric silver particles characterized by a narrow size distribution and a controlled average dimension has been obtained using a modification of the polyol process. In particular, the nanocomposite material was prepared by reduction of silver nitrate in ethylene glycol in the presence of ultrasound and PVP as a protective agent. The final particle size was controlled by removing the silver–PVP system from the reactive mixture by addition of acetone. The UV–visible spectrum of the material shows a very strong plasmon resonance band centred at 410 nm. The band position depends on the particle size and, consequently, the control of the particle growth process allows one to modulate the nanocomposite absorption wavelength. Such an important characteristic offers the possibility to use Ag–PVP nanocomposites to produce UV-absorbers and colour filters for advanced optical devices.**

**Keywords: nanocomposites; silver nanoparticles; poly(*N*-vinylpyrrolidone); polyol process; UV-absorbers; colour filters**

## 1 INTRODUCTION

Interest in condensed matter at size scales larger than atoms but much smaller than bulk solids has grown rapidly over the last few years. Matter containing from tens to thousands of atoms can have structures and properties significantly different from those of conventional materials;[1] consequently, the current research on nanostructured materials is principally devoted to the understanding of changes in the fundamental properties. Particularly interesting is the study of metal properties behaviour on a nanometric scale.[2,3] Size-dependent changes in band-gap energy, excited-state electronic behaviour, and optical spectra are generated that differ drastically from those known for the bulk limit. In addition, the new characteristics of this class of materials make them really attractive for a number of technological applications,[4–6] including photonic devices, catalysis, corrosion protection, solar energy conversion, and chemical or biochemical sensors.

Preparation and characterization of nanocrystallites is a very critical point for a fundamental understanding and tailoring of materials properties of practical use. Metal–polymer nanocomposite materials require nanometric particles with uniform size, controlled dimensions, and regular shape. Such particles can be obtained by solution chemistry (chemical precipitation and sol–gel technique) and by vapour deposition (gas evaporation, laser ablation, and sputtering).[7] However, solution chemistry is the only technique that provides a cost-effective method for the production of large quantities of nanoparticles and allows one to manipulate matter at the molecular level. Solution chemistry is the most practical route for the synthesis of nanoscale particles, but the control of size distribution, particle morphology, and crystallinity still need further investigation.

A number of metallic powders of easily reducible metals have been successfully synthesized in the

---

* Correspondence to: G. Carotenuto, Institute of Composite Materials Technology, National Research Council, Piazzale Tecchio 80, 80125 Naples, Italy.
E-mail: giancaro@unina.it

† Based on work presented at the 1st Workshop of COST 523: Nanomaterials, held 20–22 October 1999, at Frascati, Italy.

micrometre and sub-micrometre size ranges by the polyol process,[8,9] and a recent patent extends its use to the preparation of refractory metals and metal alloy powders.[10] In this process, a suitable inorganic compound is dissolved in a liquid polyol and the system is heated under stirring to a given temperature, which can reach the boiling point of the polyol. The reduction of the starting compound quantitatively yields the metal as a finely divided powder. The main feature of the reaction mechanism is that metal particles are formed by nucleation and growth from solution.[11] Because the resulting metal suspension is an almost homodisperse system, nucleation and growth are completely separated stages in the particle formation. In particular, the metal is provided slowly in solution by the progressive reduction of the dissolved species. The silver atoms concentration increases and raises the saturation concentration where the nucleation occurs. Many nuclei are produced in a short time; they grow rapidly, and the metal concentration is lowered to a point below the nucleation concentration, but high enough to allow particle growth to occur at a rate that just consumes all the metal generated. Therefore, the final micrometre-sized metal particles are formed by nuclei that have appeared spontaneously at about the same time and have grown during the same time; consequently, the particles should be very homogeneous in size. However, because of the relatively high temperature used in the synthetic process, wide Brownian motions characterize the particles and the atoms on their surface have an elevated mobility. As a result, the probability of particle collision, adhesion, and subsequent coalescence by sintering is enhanced. Particle coalescence by sintering is the means by which the system tries to attain the thermodynamic equilibrium by reducing its total surface area. Consequently, the silver powders obtained by reduction of silver nitrate in ethylene glycol are polydisperse and show a wide range of shapes, arising from the sintering of quasi-spherical individual particles. The reaction scheme for producing fine and monodisperse silver powders by the polyol process involves the reduction of the soluble silver species by ethylene glycol, nucleation of metallic silver, and growth of the individual nuclei in the presence of a suitable protective agent.[12–14] The presence of this chemical is essential for preventing the coalescence of the nuclei during the growth step. It is during the nucleation and growth steps that particle–particle adhesion and sintering must be avoided. Prevention of particle sintering can be achieved by adding a critical dosage of an organic protective agent whose function is to cover the particles, thus effectively eliminating any possibility of silver–silver particle bond formation. The presence of this agent at the solid–liquid interface does not interfere with the silver diffusion–surface deposition process, and the particles can grow to a definite size. A number of polymers can be used as protective agents (e.g. poly(vinylalcohol), poly(methylvinylether), sodium polyacrylate, poly(*N*-vinylpyrrolidone) (PVP));[15] such a component allows one to recover the fine particles as a polymer-based composite.

In this investigation, a method to obtain a polymer filled by highly monodispersed silver particles with a controlled size using ethylene glycol as a reducing agent has been developed. In particular, the polymer–colloidal silver systems were prepared from ethylene glycol solutions of silver nitrate and PVP in the presence of sonication. The Ag–PVP nanocomposite samples were characterized by transmission electron microscopy (TEM), powder X-ray diffraction (XRD), UV–visible spectroscopy, and thermogravimetric analysis (TGA).

## 2 EXPERIMENTAL

Silver nitrate (Aldrich) was the starting material for the silver nanoparticle preparation. Reagent-grade ethylene glycol (Aldrich) was used as a solvent and reducing agent for $AgNO_3$, and PVP (Aldrich, $\bar{M}_W = 10\ 000$) was used as a protective agent. All reagents were used without further purification. PVP was dissolved in ethylene glycol at room temperature, and to this solution the required amount of an $AgNO_3$–ethylene glycol solution was added quickly under sonication (Ultrasonic Cleaner, J.P. Selecta, 40 kHz). Sonication was applied during the whole reaction, which proceeds at room temperature. The reaction was also performed by dissolving at room temperature solid $AgNO_3$ in a PVP–ethylene glycol solution without subsequent stirring or sonication. The compositions used and reaction times are given in Table 1. When the colloidal dispersion had a yellow or red colour, the system was easily separated from the ethylene glycol by addition of a large amount of acetone (1:5 by volume respectively) followed by sonication and centrifugation. The PVP–Ag nanocomposites were redispersed in ethyl alcohol and precipitated again by acetone addition for purification. A schematic representation of the nanocomposite preparation

**Table 1** Compositions and reaction times used for the nanocomposite synthesis

| Sample | PVP (g) | $AgNO_3$ (mg) | $C_2H_6O_2$ (ml) | Reaction time (h) | Colour |
|---|---|---|---|---|---|
| 1 | 1.728 | 86.9 | 130 | 24 | dark yellow |
| 2 | 1.728 | 44.5 | 65 | 24 | yellow |
| 3 | 3.456 | 22.6 | 32 | 24 | red |

process is shown in Fig. 1. Optical filter prototypes (see Plate 1) were obtained by placing an Ag–PVP–ethanol paste between two polycarbonate plates and then removing the ethanol by heating in oven at 60 °C under vacuum. Finally, the plate edges were sealed with a silicone resin.

XRD data were collected on a Philips powder diffractometer (PW1710) with Cu K$\alpha_1$ radiation, using Philips-APD software. The data were collected between 10 and 80 ° in steps of 0.02 ° and a dwell time of 1 s.

The silver nanoparticle morphology was characterized by TEM (Philips-CM12 microscope). Samples for observation in the microscope were prepared by placing a drop of the colloidal silver dispersion onto a standard microscope grid coated with a carbon film. The mean particle size of the colloidal silver dispersions and the standard deviation of the particle population were determined by image analysis of the TEM micrographs.

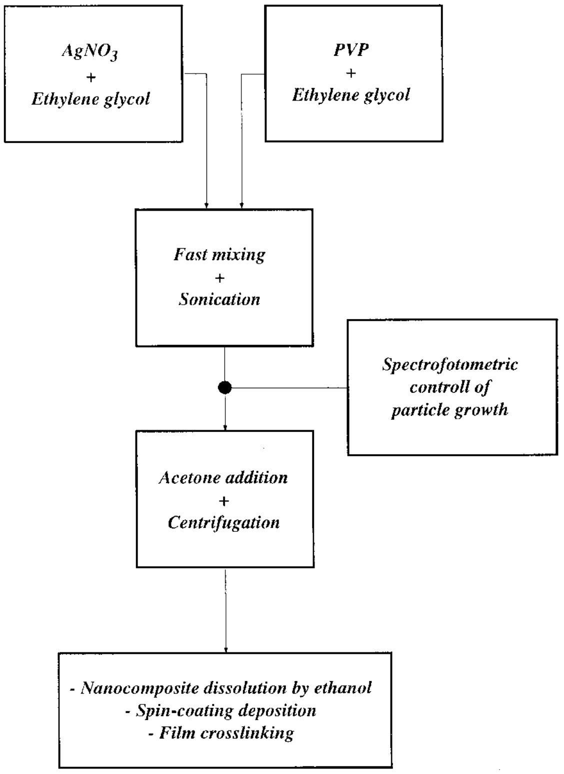

**Figure 1** Schematic representation of the nanocomposite film preparation process.

The UV–visible absorption spectra of the nanocomposite samples were obtained using a UVIKON 930 UV-spectrophotometer (Kontron Instruments) with a variable radiation wavelength between 300 and 800 nm.

## 3 RESULTS

The microstructure of silver particles contained in thin nanocomposite films was analysed by TEM. All particles obtained by direct mixing $AgNO_3$ with PVP–ethylene glycol solution in the absence of sonication had a pseudo-spherical shape, which became more regular for smaller particles (see Fig. 2a). Aggregates or particles sintered together were not present in the composite material. The particle size was polydispersed with a diameter ranging from 4 to 30 nm. In particular, the size distribution was monomodal and can be described by a Gaussian function with $\mu = 12$ nm and $\sigma = 4.6$ nm (see Fig. 2b). Since the diameter of a silver atom is 2.88 Å, the smallest particles contained less than 3000 atoms of silver. The particle size was less than the visible light wavelength; therefore, no particle was able to contribute to light scattering phenomena and the resulting nanocomposite was transparent.

As shown in Fig. 2a, for most of the silver particles the pseudo-spherical shape corresponded to a polyhedron, and it was possible to observe that some particles were representable schematically as a decahedron. Other particles observed exhibited an icosahedron shape. Such an observation is in agreement with those reported in the literature and prove that our particles are monocrystalline and polyhedral. There are two conflicting views for the structure of small metal particles.[16] They can be

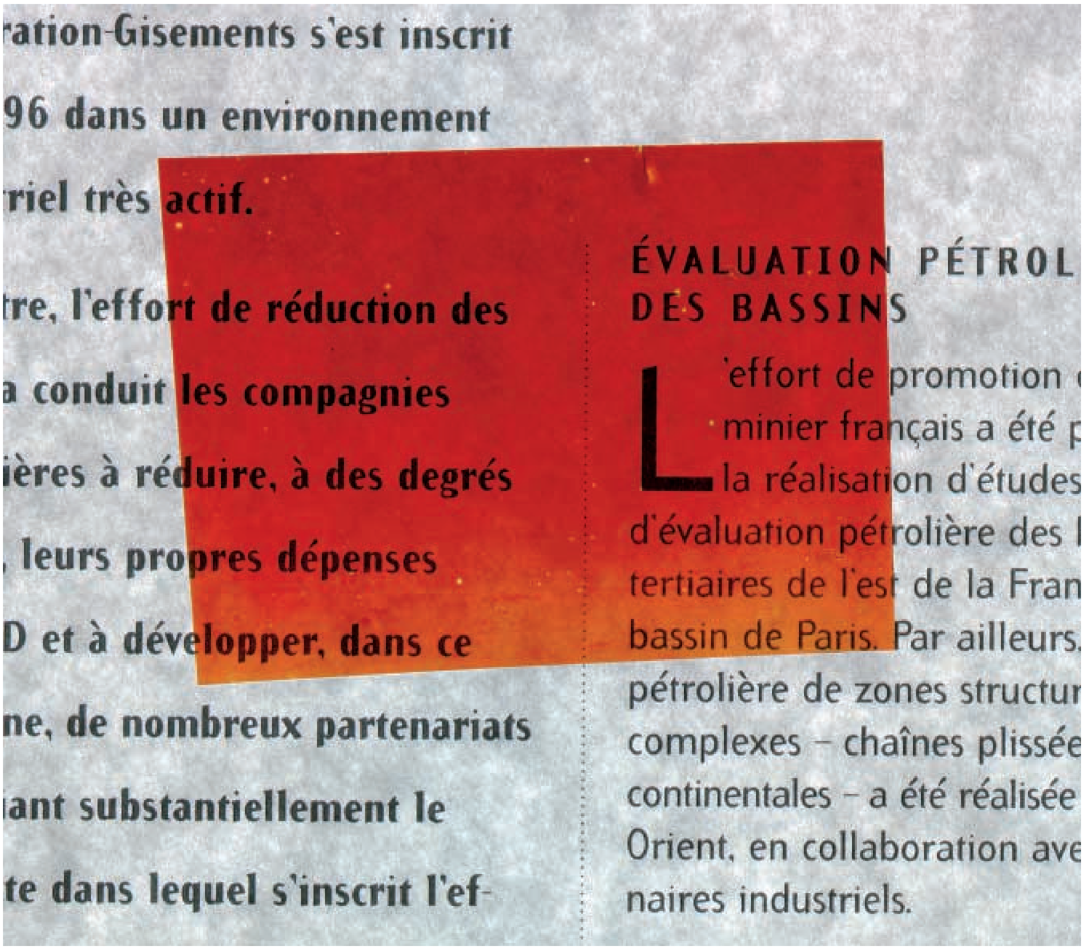

ration-Gisements s'est inscrit
96 dans un environnement
riel très actif.
tre, l'effort de réduction des
a conduit les compagnies
ières à réduire, à des degrés
, leurs propres dépenses
D et à développer, dans ce
ne, de nombreux partenariats
iant substantiellement le
te dans lequel s'inscrit l'ef-

ÉVALUATION PÉTROL
DES BASSINS

L'effort de promotion
minier français a été p
la réalisation d'études
d'évaluation pétrolière des l
tertiaires de l'est de la Fran
bassin de Paris. Par ailleurs,
pétrolière de zones structur
complexes – chaînes plissée
continentales – a été réalisée
Orient, en collaboration ave
naires industriels.

**Plate 1** Optical filter made of silver nanoparticles dispersed in a PVP matrix (8 wt% silver). The film is heavily red coloured but also highly transparent.

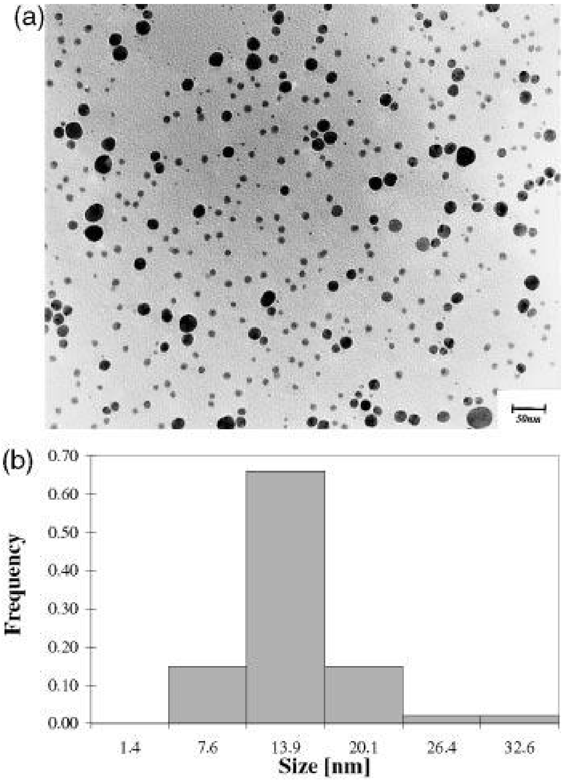

**Figure 2** TEM micrograph (a), and size distribution (b) of silver nanoparticles obtained by dissolving $AgNO_3$ in PVP–glycol solution without subsequent sonication treatment.

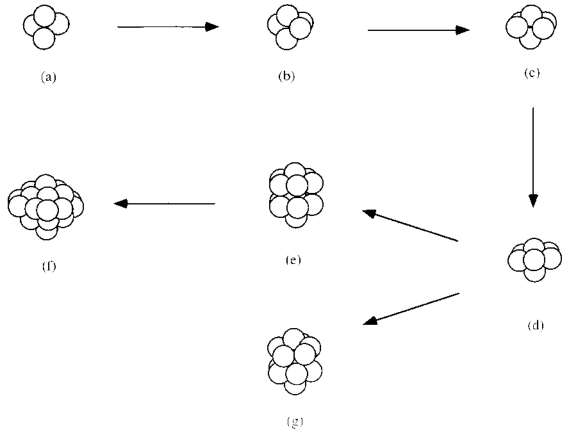

**Figure 3** Schematic representation of a possible particle growth mechanism. Successive addition of single atoms to a tetrahedral cluster (a) leads to a trigonal bipyramid (b), a capped bipyramid (c), and a simple decahedron or pentagonal bipyramid (d). Further addition of atoms in normal metallic packing leads to the development of the decahedron (e) and (f), or, if tetrahedral packing is maintained, to the icosahedron (g).

regarded as having the same structures as bulk metals with changes in properties arising from the gradual loss of a long-range translational lattice as the particle size is reduced, or they can be considered as produced by growth from nuclei with a structure fundamentally different from that of bulk metal. In particular, according to the scheme illustrated in Fig. 3, the construction of a lattice can take place by successive addition of individual metal atoms to a simple tetrahedral unit. A growth process of this type can explain the formation of the polyhedral particles found in the microcrystalline metals prepared by the present method, and suggests that the structure and electronic properties of very small crystallites (clusters) may be significantly different from those of the bulk metals.

As shown in Fig. 4a and b, when the silver particles were obtained by fast mixing of two precursor solutions, each including just one of the required reagents, and the reaction was performed in presence of sonication (or strong stirring), a highly homodisperse product was obtained. In particular, the particle size ranges between 3 and 9 nm and can be described by a Gaussian function with $\mu = 5.7$ nm and $\sigma = 1.3$ nm. In this case a single nucleation stage takes place during the nanochemical process and the nucleation period is shorter than without sonication (see Fig. 5). A very uniform particle size distribution is of primary importance in the preparation of a material to be used as pigment for colour filters and UV-absorbers, because in this case all particles can absorb at the same wavelength.

Nanocomposite films were characterized by UV–visible spectroscopy. Figure 6 depicts the optical spectrum of metal particles at two different concentrations. The presence of silver(0) in solution is related to a broad and strong absorbance peak whose maximum occurs at 410 nm. The silver content can be determined by measuring the peak height in the UV–visible spectra of the nanocomposite. According to Mie theory, the optical absorption and scattering of metal particles are due to the excitation of surface plasmons of small metal particles by an external oscillating electric field.[17–19] When the particle size is small enough compared with the wavelength of light, their optical spectra are predominantly attributed to light absorption by dipole polarization of particles. For bulk metals these resonant wavelengths are usually located in the IR portion of the spectrum. However,

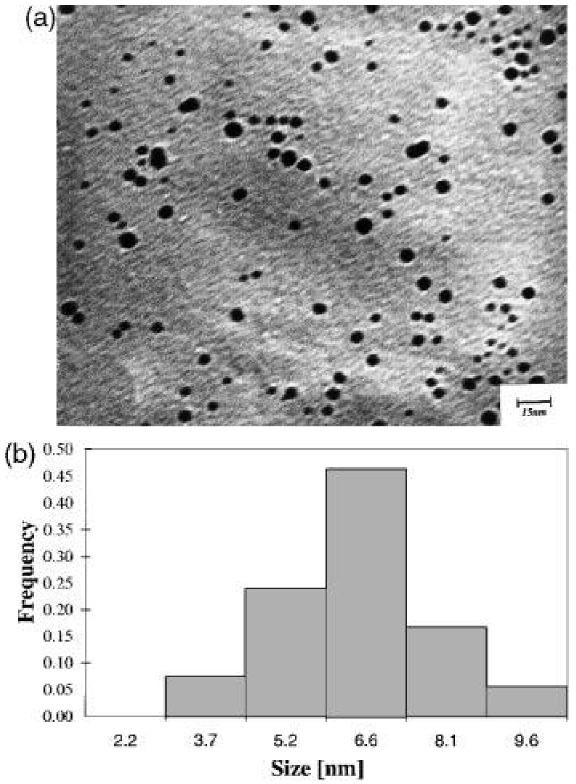

**Figure 4** TEM micrograph (a) and size distribution (b) of silver nanoparticles obtained by 'fast mixing' of the precursor solutions followed by sonication.

when these materials are fabricated as small as nanoparticles the gap between the excitation bands is widened. A widened gap will absorb a photon of a higher energy level (visible spectrum). In the analysis of the maximum absorption wavelength of the surface plasmon band, the effects of particle size, aggregation state, metal composition, surface adsorption layer, etc. should also be considered.

XRD patterns of the colloidal silver dispersions were taken. The colloidal silver obtained was crystalline and produced an XRD pattern characteristic of silver. Figure 7 shows a typical example of such a diffraction pattern in comparison with the XRD pattern of pure silver. The value of the lattice constant was calculated from its corresponding XRD pattern: $a = 4.078$ Å, which is consistent with the value of $a = 4.0862$ Å given by the JCPDS file no. 4-0783. The nanoparticles always exhibit a good crystallinity. The mathematical deconvolution of the peaks by a Lorentz function permitted a better calculation of the peak parameters that were used to measure the crystallite sizes using the

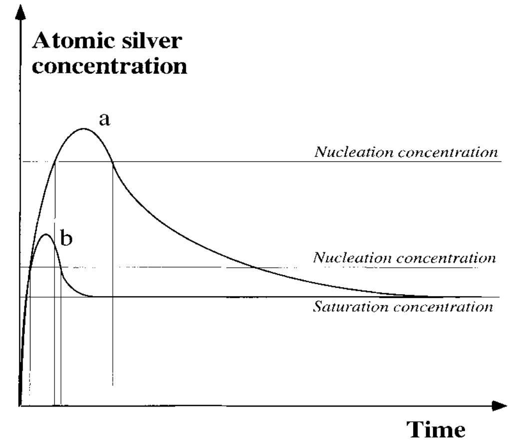

**Figure 5** Atomic silver concentration *versus* time in the absence (a), and in the presence (b) of strong agitation (stirring or sonication).

Scherrer formula:

$$d = \frac{k\lambda}{\beta_{1/2}\cos\theta} \qquad [1]$$

where $\beta_{1/2}$ is the full-width at half maximum of the peak at $2\theta$, $k$ is a constant ($k = 0.89$), and $\lambda = 54060$ Å is the Cu K$\alpha_1$ wavelength.

The results for the (111)* direction, using the sample in Fig. 2, is a crystallite size of 11 nm. Although the Scherrer formula always tends to underestimate the real crystallite size, this value is very close to the TEM result and, consequently, each particle should be a single crystal.

Finally, the reaction yield was obtained from the

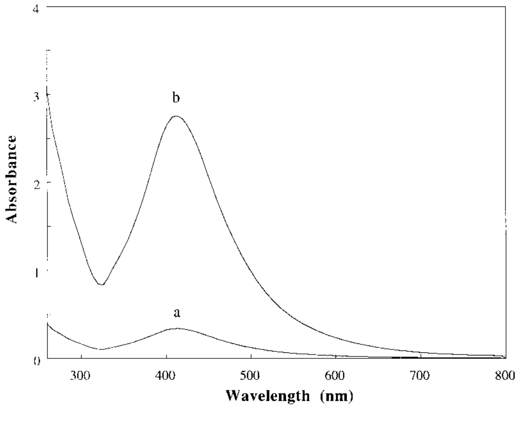

**Figure 6** UV–visible spectra of Ag–PVP nanocomposite films: (a) 2 wt% silver; (b) 5 wt% silver.

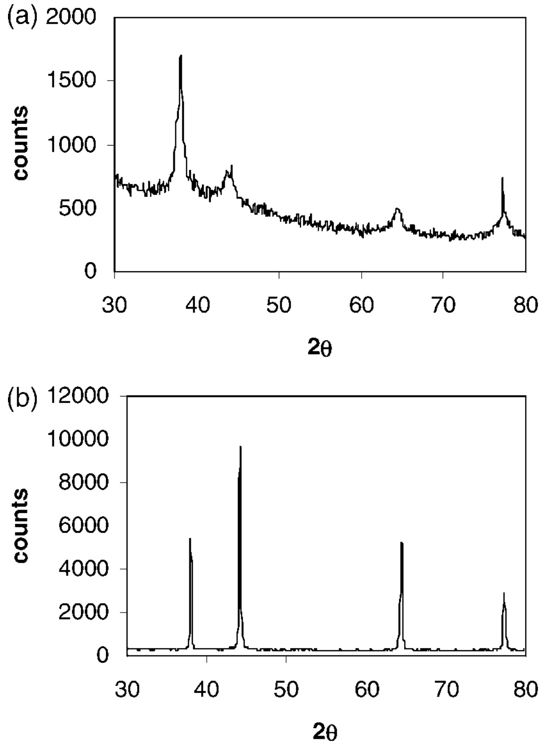

**Figure 7** XRD patterns of: (a) silver-cluster–PVP nanocomposite and (b) pure silver (sheet with oriented grains).

weight percent of silver particles incorporated in the polymer, which was estimated by TGA of nanocomposite samples in flowing nitrogen. Usually, the polymer decomposition was visible at temperatures higher than 400 °C, and the silver content for the experimental conditions reported in Table 1 was approximately 8% by weight.

## 4 DISCUSSION

As shown in Fig. 4, after the nucleation stage, which is very short in the presence of sonication, the concentration of atomic silver present in the solution is reduced to the saturation concentration and the particle growth process is controlled by the rate of the chemical reaction and the diffusion of silver atoms from the solution to the nucleus surfaces. Because of the silver surface plasmon absorption, it is possible to see a slow chromatic evolution in the reactive mixture, which can be used for monitoring the particle growth and to stop the process at the nanometre-sized level. Practically, the same synthetic process can be used to prepare silver clusters, nanoparticles and sub-micrometric particles.

In particular, the silver colloid can be promptly separated from the ethylene glycol–$AgNO_3$ solution by addition of a large amount of acetone. This extraction of nanosized silver particles is based on the PVP precipitation by a mixture of two miscible solvents differing by their ability to dissolve the polymer. The polymer bonded to the silver particles is highly soluble in ethylene glycol and very poorly soluble in acetone. Consequently, a progressive addition of acetone to the PVP–silver suspension causes, at a given volume of added acetone, the system to become cloudy and a precipitate appears. This situation corresponds to the agglomeration of the PVP–silver system as a result of their greater van der Waals interactions. Ethylene glycol and unreacted $AgNO_3$ are soluble in acetone and, therefore, they can be completely separated from the silver particles. In addition, at room temperature the reduction reaction becomes completely stopped because of the absence of PVP in the acetone medium.

The possibility of preparing a polymer-based nanocomposite material, that includes highly homodisperse silver particles, the average size of which can be accurately controlled, is very important in the preparation of colour filters and absorbers able to remove radiation of specific wavelengths. The colloidal silver polychromism is observed because, in the condensation of metal atoms to form a solid, the first stage is characterized more by molecular-like properties than by metallic characteristics. The one-electron energy levels, the number of which is of the order of the number of atoms in the cluster, have not yet formed energy bands, but are discrete. Hence the valence electrons cannot be continuously accelerated by an external electric field and are only able to change their energy through transitions between quantized eigenstates. Changes of the electronic properties of particles caused by the discreteness of the energy levels is of the order:

$$\Delta E \approx \frac{\varepsilon_F}{Z} \qquad [2]$$

where $\varepsilon_F$ is the Fermi energy and $Z$ the number of atoms in the particle. It has been pointed out that these discrete electron eigenstates will be broadened by lifetime limitation. This broadening may possibly increase with increasing particle size. Quantum-size effects vanish in particles where the energy level broadening $\delta E$ exceeds the mean spacing $\Delta E$ between the levels. Since $\Delta E$ depends on the particle size $d$, a critical diameter $d_c$ can be defined with:

$$d < d_c \quad \delta E < \Delta E \quad \text{(quantum size region)}$$

$$d > d_c \; \delta E > \Delta E \; \text{(quasi-continuous energy bands)}$$

Consequently, in the preparation of metal nanoparticles to be used as pigments for colour filters or UV-absorbers, it is very important to be able to control the particle size, so as to produce particles with a diameter inferior to the critical value $d_c$.

The critical diameter is a function of temperature and depends on the method of particle preparation, because both $\Delta E$ and $\delta E$ may be influenced by the particle shape, the crystalline structure, and the nature of the embedding matrix. In particular, a drastic decrease in the extinction coefficient of the plasmon band is produced by PVP because the polar amide groups, present in the individual polymer unit, have a strong affinity for the metallic silver and, therefore, are strongly bonded to its surface. This strong decrease in the intensity and the red-shift of the band maximum observable in the absorption spectrum of coated particles are due to a change in the free-electron density, which induces changes in the surface plasmon band of silver particles, and yields a variation of the width and maximum of the plasmon band absorption. In particular, the chemisorption of a nucleophilic molecule on the silver surface is accompanied by a charge donation to the metal. The cumulative effect of the adsorption of many molecules produces a positive shift of the Fermi level energy. This shift is very important in the control of nanocomposite absorption wavelengths, and it can be easily related to parameters characteristic of the particle chemical environment, on the basis of the free-electron gas approximation. In this case, the Fermi energy $\varepsilon_F$ of a metal nanoparticle is related to its volume $V$, and the total number of valence shell electrons $N_e$ (i.e. the electron density) by the following equation:

$$\varepsilon_F = \frac{\hbar^2}{2m_e} \cdot \left(3\pi^2 \frac{N_e}{V}\right)^{2/3} \qquad [3]$$

where $m_e$ is the electron mass. An increase of $N_e$ by a small fraction produces a change of the Fermi energy given by

$$\Delta\varepsilon_F = \frac{2}{3}\varepsilon_F \frac{\Delta N_e}{N_e} \qquad [4]$$

$\Delta N_e$ can be expressed as the product of the number of nucleophilic molecules of adsorbate directly bonded to the particle surface and the fractional charge associated with each chemisorption bond $\delta_e$. $\Delta\varepsilon_F$ can therefore be written as:

$$\Delta\varepsilon_F = \frac{2}{3}\varepsilon_F x \left(\frac{n_s}{N}\right)\delta_e \qquad [5]$$

where $n_s$ is the number of silver atoms present on the surface of a particle, $x$ is the fraction of this atoms that are bonded to adsorbate molecules, and $N$ ($N = N_e$ for silver, being Ag:[Kr]$4d^{10}5s^1$) is the total number of atoms contained in a particle. Equation [5] shows that the positive shift of the Fermi level energy is proportional to the fractional charge donated by the ligand, the fraction of particle surface occupied by ligand molecules, and particle surface–volume ratio. In particular, $\delta_e$ is an effective charge, a function of the ligand charge and silver–ligand affinity, and $x$ is principally related to the ligand concentration. In the case of a spherical particle with radius $R$, the $n_s/N$ quantity can be easily expressed as a function of particle and atom size:

$$\frac{n_s}{N} = \frac{4r}{R} \qquad [6]$$

where $r$ is the silver atom radius. Finally, $\Delta\varepsilon_F$ can be written as:

$$\Delta\varepsilon_F = k\frac{x\delta_e}{R} \qquad [7]$$

with $k = (8/3)\varepsilon_F r$. Therefore, $\Delta\varepsilon_F$ increases significantly with decrease of particle size, and for silver clusters, the diameters of which are a few nanometres, an appreciable shift of the Fermi level can be observed as an effect of the nucleophilic molecule adsorption.

Such a point is very important, because the use of protective agents differing from PVP (e.g. poly(vinylalcohol), poly(methylvinylether), etc.) allows the preparation of silver-based colour filters with absorption bands located at different wavelengths. Thin films of silver nanocomposite containing polymers of a different nature can be overlapped, producing a multilayer structure able to absorb radiation over a wide range of wavelengths.

## 5 CONCLUSIONS

The preparation of polymer-based nanocomposites by chemical routes has the advantages of: (a) a size control at the cluster level; and (b) an efficient scale-up for processing and production. Here, a new method for the direct preparation of Ag–PVP nanocomposite materials with a controlled and highly homodispersed filler size has been developed. The method uses ethylene glycol as a reducing agent for $AgNO_3$ and PVP to prevent particle sintering. The reaction was carried out in the presence of sonication at room temperature and the process of particle growth was terminated by acetone addition. The microscopical characterization of the nanocomposite samples shows that the use of sonication during the synthetic process performed at room temperature allows one to obtain silver clusters with a uniform size distribution. A more uniform distribution should be obtainable by increasing the temperature; however, in this case the reaction rate is high and the particle growth process is difficult to stop at the cluster level.

## REFERENCES

1. Kojarnovitch V (ed.). *New and Advanced Materials, Emerging Technologies Series*. United Nations Industrial Development Organization: Vienna, 1997.
2. Ashoori RC. *Nature* 1996; **379**: 413–419.
3. Allen GL, Bayles RA, Gile WW, Jesser WA. *Thin Solid Films* 1986; **144**: 297–308.
4. Weibel M, Caseri W, Suter UW, Kiess H, Wehrli E. *Polym. Adv. Technol.* 1991; **2**: 75–80.
5. Zimmermann L, Weibel M, Caseri W, Suter UW, Walther P. *Polym. Adv. Technol.* 1992; **4**: 1–7.
6. Zimmermann L, Weibel M, Caseri W, Suter UW. *J. Mater. Res.* 1993; **8**(7): 1742–1748.
7. Subramanian R, Denney PE, Singh J, Otooni M. *J. Mater. Sci.* 1998; **33**: 3471–3477.
8. Fievet F, Lagier JP, Blin B, Beaudoin B, Figlarz M. *Solid State Ionics* 1989; **32–33**: 198–205.
9. Fievet F, Lagier JP, Figlarz M. *MRS Bull.* 1989; **14**(12): 29–34.
10. US Patent 5 922 409, July 13, 1999.
11. LaMer VK, Dinegar RH. *J. Am. Chem. Soc.* 1950; **72**: 4847–4854.
12. Ducamp-Sanguesa C, Herrera-Urbina R, Figlarz M. *J. Solid State Chem.* 1992; **100**: 272–280.
13. Silvert PY, Herrera-Urbina R, Duvauchelle N, Vijayakrishnan V, Elhsissen KT. *J. Mater. Chem.* 1996; **6**(4): 573–577.
14. Silvert PY, Herrera-Urbina R, Elhsissen KT. *J. Mater. Chem.* 1997; **7**(2): 293–299.
15. Meguero K, Nakamura Y, Hayashi Y, Torizuka M, Esumi K. *Bull. Chem. Soc. Jpn.* 1988; **61**: 347–350.
16. Duff DG, Curtis C, Edwards PP, Jefferson DA, Johnson BFG, Logan DE. *J. Chem. Soc. Chem. Commun.* 1987; **3**: 1264–1266.
17. Kreibig U. *J. Phys. F: Met. Phys.* 1974; **4**: 999–1014.
18. Genzel L, Martin TP, Kreibig U. *Z. Phys. B* 1975; **21**: 339–346.
19. Charlé KP, Rank FF, Shulze W. *Ber. Bunsenges. Phys. Chem.* 1984; **88**: 350–354.